Big-bang nucleosynthesis with unstable gravitino and upper bound on the reheating temperature

Kazunori Kohri,[1,2] Takeo Moroi,[3] and Akira Yotsuyanagi[3]

[1]*Harvard-Smithsonian Center for Astrophysics, 60 Garden Street Cambridge, Massachusetts 02138, USA*

[2]*Department of Earth and Space Science, Graduate School of Science Osaka University, Toyonaka 560-0043, Japan*

[3]*Department of Physics, Tohoku University, Sendai 980-8578, Japan*

(Received 8 August 2005; published 8 June 2006)

We study the effects of unstable gravitino on big-bang nucleosynthesis. If the gravitino mass is smaller than $\sim$10 TeV, primordial gravitinos produced after inflation are likely to decay after big-bang nucleosynthesis starts, and light-element abundances may be significantly affected by hadro and photodissociation processes as well as by $p \leftrightarrow n$ conversion process. We calculate the light-element abundances and derive upper bounds on the reheating temperature after inflation. In our analysis, we calculate decay parameters of the gravitino (i.e. lifetime and branching ratios) in detail. In addition, we perform a systematic study of the hadron spectrum produced by the gravitino decay, taking account of all the hadrons produced by the decay products of the gravitino (including the daughter superparticles). We discuss model dependence of the upper bound on the reheating temperature.

DOI: 10.1103/PhysRevD.73.123511 PACS numbers: 26.35.+c, 12.60.Jv, 98.80.Cq, 98.80.Ft

I. INTRODUCTION

Low-energy supersymmetry, which is one of the most prominent candidates of the physics beyond the standard model, may significantly affect the evolution of the Universe. One reason is that, assuming R-parity conservation, the lightest superparticle (LSP) is stable, which becomes a well-motivated candidate of the cold dark matter. Another reason, which is very important in the framework of local supersymmetry (i.e. supergravity), is that there exists various very weakly interacting particles. The most important example is the gravitino, which is the gauge field for the local supersymmetry.

Since the gravitino is the superpartner of the graviton, its interaction is suppressed by inverse powers of the gravitational scale and hence its interaction is very weak. Even though the gravitino is very weakly interacting, it can be produced by scattering processes between standard model particles (and their superpartners) in the thermal bath in the early Universe. Once produced, the gravitino decays with a very long lifetime. In particular, if the gravitino mass is smaller than $\sim$20 TeV, the lifetime becomes longer than $\sim$1 sec and hence the primordial gravitinos decay after big-bang nucleosynthesis (BBN) starts. The (unstable) gravitino is expected to be relatively heavy, and its decay releases energetic particles which cause dissociation processes of the light elements generated by the standard BBN reactions. Since the standard BBN scenario generally predicts light-element abundances consistent with observations, these dissociation processes modify the light-element predictions and can potentially destroy this concordance. Comparisons between these new predictions and observations provide significant constraints on the primordial abundance of the gravitino [1].[1]

In the inflationary scenario, which is also strongly suggested by the Wilkinson Microwave Anisotropy Probe (WMAP) data [4], gravitinos are diluted by the entropy production after inflation. However, even in this case, gravitinos are produced again by scattering processes of the particles in the thermal bath. Importantly, the total amount of the gravitino produced by the scattering is approximately proportional to the reheating temperature T_R. Thus, if the reheating temperature is too high, the gravitino abundance becomes so large that the light-element abundances are too much affected to be consistent with observations. In the past, the BBN constraints on the unstable gravitino have been intensively studied [5–17].[2]

Recently, Kawasaki and two of the present authors (K. K. and T. M.) have studied the constraints on the unstable long-lived particles from BBN in detail [15,16]; in particular, in this paper, effects of the hadrons produced by the decay of such unstable particles (as well as the effects of photodissociation) were systematically studied,[3] and general constraints on the primordial abundance of such unstable particles were presented. Then, the results were applied to the case of the unstable gravitino and the upper bound on the reheating temperature was obtained for several simple cases.

In [15,16], however, several simplifications and assumptions are made for the properties of the gravitino. First of all, several very simple decay patterns of the gravitino were considered, which are applicable for very specific mass

[1]Constraints on the case with the gravitino LSP have been considered in Refs. [2,3].

[2]In order to relax the constraints, several scenarios have been studied. In Ref. [18], it was discussed that the modification of the expansion rate by the 5D effect in the braneworld cosmology, which may reduce the abundance of the gravitino. In Ref. [19], they studied possibilities of the dilution of the gravitino by the late-time entropy production due to the decaying moduli without newly producing many gravitinos.

[3]For old studies on the effects of the hadronic decay modes, see also [20,21].

spectrum of the superparticles. In addition, for the hadronic branching ratio of the gravitino, only several typical values were used to obtain the constraint. Furthermore, for some cases (in particular, for the case where the gravitino dominantly decays into the gluon and the gluino), effects of the hadrons emitted from the superparticles (like the gluino) were neglected. Thus, it is desirable to perform a more detailed and complete analysis of the upper bound on the reheating temperature with the unstable gravitino.

In this paper, we study the effects of unstable gravitinos on BBN, paying particular attention to the properties of the gravitino. Compared to previous works, decay processes of the gravitino (and decay chains of the decay products including the superparticles) are precisely and systematically studied. As a result, energy spectra of the hadrons (in particular, proton, neutron, and pions) produced by the gravitino decay are studied in detail for various mass spectrum of the superparticles.

The organization of this paper is as follows. In Sec. II, we present the model we consider and summarize the important parameters for our analysis. In Sec. III, detail of the decay processes of the gravitino is discussed. Some of the important issues in our analysis, which is the secondary decays of the daughter particles from the gravitino decay and their hadronization processes, are discussed in Sec. IV. Then, in Sec. V, the outline of our calculation of the light-element abundances is discussed. Our main results are given in Sec. VI, and Sec. VII is devoted for conclusions and discussion.

II. MODEL

In this paper, we adopt the minimal particle content to derive the upper bound on the reheating temperature. Thus, the model we consider includes the particles in the minimal supersymmetric standard model (MSSM) as well as the gravitino. These particles are listed in Table I.

In order to precisely calculate the decay rate of the gravitino, it is necessary to obtain the mass eigenvalues and mixing parameters of the superparticles. Thus, we briefly summarize the relation between the gauge-eigenstate and mass-eigenstate bases here.

We start with the neutralino sector. With the $SU(2)_L$ and $U(1)_Y$ gaugino masses M_2 and M_1 as well as the supersymmetric Higgs mass μ_H, the mass matrix of the neutralinos is given in the form[4]

$$\mathcal{M}_{\chi^0} = \begin{pmatrix} M_1 & 0 & -m_Z \sin\theta_W \cos\beta & m_Z \sin\theta_W \sin\beta \\ 0 & M_2 & m_Z \cos\theta_W \cos\beta & -m_Z \cos\theta_W \sin\beta \\ -m_Z \sin\theta_W \cos\beta & m_Z \cos\theta_W \cos\beta & 0 & -\mu_H \\ m_Z \sin\theta_W \sin\beta & -m_Z \cos\theta_W \sin\beta & -\mu_H & 0 \end{pmatrix}, \tag{2.1}$$

where m_Z is the Z-boson mass while θ_W is the weak mixing angle, and $\tan\beta$ is the ratio of the vacuum expectation values of up and down-type Higgs bosons. This mass matrix is diagonalized by a unitary matrix U_{χ^0} as

$$U^*_{\chi^0} \mathcal{M}_{\chi^0} U^{-1}_{\chi^0} = \mathrm{diag}(m_{\chi^0_1}, m_{\chi^0_2}, m_{\chi^0_3}, m_{\chi^0_4}). \tag{2.2}$$

In addition, for the chargino sector, the mass matrix is given by

$$\mathcal{M}_{\chi^\pm} = \begin{pmatrix} M_2 & \sqrt{2} m_W \cos\beta \\ \sqrt{2} m_W \sin\beta & \mu_H \end{pmatrix}, \tag{2.3}$$

where m_W is the $W^\pm$-boson mass. We define the unitary matrices diagonalizing $\mathcal{M}_{\chi^\pm}$ as U_{χ^+} and U_{χ^-}:

$$U^*_{\chi^+} \mathcal{M}_{\chi^\pm} U^{-1}_{\chi^-} = \mathrm{diag}(m_{\chi^\pm_1}, m_{\chi^\pm_2}). \tag{2.4}$$

For the neutral Higgs boson, the gauge eigenstates (i.e., the up-type Higgs H^0_u and down-type Higgs H^0_d) and the mass eigenstates are related by using the mixing angle α:

$$\begin{pmatrix} H \\ h \end{pmatrix} = \sqrt{2} \begin{pmatrix} \cos\alpha & \sin\alpha \\ -\sin\alpha & \cos\alpha \end{pmatrix} \begin{pmatrix} \mathrm{Re}(H^0_d) - v_1 \\ \mathrm{Re}(H^0_u) - v_2 \end{pmatrix}, \tag{2.5}$$

where v_1 and v_2 are vacuum expectation values of H^0_d and H^0_u, respectively.

In addition, we have to consider the mixings in the squark and slepton mass matrices. For simplicity, we do not consider the generation mixing in the squark and slepton sector. We also neglect the left-right mixing in the first and second generation squarks and sleptons since such mixing is small in many classes of models, in particular, in the minimal supergravity (mSUGRA) type models which we adopt in our analysis. For the third-generation squarks and sleptons, we take account of the effects of the left-right mixing. Such mixing is parametrized by unitary matrices $U_{\tilde{t}}$, $U_{\tilde{b}}$, and $U_{\tilde{\tau}}$ which diagonalize the mass-squared matrices of the squarks and sleptons:

$$U_{\tilde{f}} \mathcal{M}^2_{\tilde{f}} U^{-1}_{\tilde{f}} = \mathrm{diag}(m^2_{\tilde{f}_1}, m^2_{\tilde{f}_2}): \tilde{f} = \tilde{t}, \tilde{b}, \tilde{\tau}. \tag{2.6}$$

In our analysis, we consider the case where the gravitino is unstable and the LSP is one of the MSSM particles. Since the charged or colored LSP is disfavored, we consider the case where the LSP is the lightest neutralino χ^0_1. Consequently, the gravitino is assumed to be heavier than χ^0_1. Of course, the gravitino may be heavier than other superparticles and hence the lifetime and branching ratios for possible decay modes of the gravitino depend on the

[4]We used the convention of [22].

TABLE I. List of particles in the mass-eigenstate bases.

Particles	Notation
Gravitino	ψ_μ
Neutralinos	χ_1^0, χ_2^0, χ_3^0, χ_4^0
Charginos	$\chi_1^\pm$, $\chi_2^\pm$
Gluino	$\tilde{g}$
Squarks	$\tilde{q} = \tilde{u}_L$, $\tilde{u}_R$, $\tilde{d}_L$, $\tilde{d}_R$, $\tilde{s}_L$, $\tilde{s}_R$, $\tilde{c}_L$, $\tilde{c}_R$, $\tilde{b}_1$, $\tilde{b}_2$, $\tilde{t}_1$, $\tilde{t}_2$
Sleptons	$\tilde{e}_L$, $\tilde{e}_R$, $\tilde{\mu}_L$, $\tilde{\mu}_R$, $\tilde{\tau}_1$, $\tilde{\tau}_2$, $\tilde{\nu}_{e_L}$, $\tilde{\nu}_{\mu_L}$, $\tilde{\nu}_{\tau_L}$
Photon	γ
Weak bosons	Z, $W^\pm$
Gluon	g
Neutral CP-even Higgs	h, H
CP-odd Higgs	A
Charged Higgs	$H^\pm$
Quarks	$q = u$, d, s, c, b, t
Leptons	e, μ, τ, ν_e, ν_μ, ν_τ

mass spectrum. We calculate these quantities in detail, as we explain below.

In order to calculate the decay rate of the gravitino, it is necessary to fix the mass spectrum and the mixing matrices in the MSSM sector. Although the effects of the gravitino on BBN can be calculated for arbitrary mass spectrum of the MSSM particles, it is not practical to study all the possible cases since there is a very large number of parameters in the MSSM sector. Thus, we adopt a simple parametrization of the SUSY breaking parameters, that is, the mSUGRA-type parametrization of the soft SUSY breaking parameters. We parametrize the MSSM parameters by using unified gaugino mass $m_{1/2}$, universal scalar mass m_0, universal coefficient for the trilinear scalar coupling A_0, ratio of the vacuum expectation values of two Higgs bosons $\tan\beta$, and supersymmetric Higgs mass μ_H (for the details, see reference of [23]). Then, the properties of the superparticles (including the gravitino) are determined once these parameters as well as the gravitino mass $m_{3/2}$ are fixed and, consequently, we can derive the upper bound on the reheating temperature. Notice that, although we adopt the simple parametrization of the soft SUSY breaking parameters, our analysis is applicable to more general cases as far as the gravitino is heavier than one of the MSSM superparticles (like the lightest neutralino).

TABLE II. mSUGRA parameters used in our analysis.

	Case 1	Case 2	Case 3	Case 4
$m_{1/2}$	300 GeV	600 GeV	300 GeV	1200 GeV
m_0	141 GeV	218 GeV	2397 GeV	800 GeV
A_0	0	0	0	0
$\tan\beta$	30	30	30	45
μ_H	389 GeV	726 GeV	231 GeV	-1315 GeV
$m_{\chi_1^0}$	117 GeV	244 GeV	116 GeV	509 GeV
$\Omega_{\rm LSP}^{\rm (thermal)}h^2$	0.111	0.110	0.106	0.111

Even with the mSUGRA parametrization of the MSSM parameters, the whole parameter space is still too large to be completely studied. Thus, in this paper, we consider several typical mSUGRA points and derive constraints for these points. In particular, we pick up the points where the thermal relic density of the LSP becomes consistent with the dark matter density determined by the WMAP observation [4]. The points we consider are listed in Table II. For all the cases, we checked that the lightest neutralino becomes the LSP (if the gravitino mass is larger than $m_{\chi_1^0}$). Using DarkSUSY package [24], we calculated the thermal relic density of the LSP $\Omega_{\rm LSP}^{\rm (thermal)}$.[5] (We use $h = 0.71$ [4], where h is the expansion rate of the Universe in units of 100 km/ sec /Mpc.)

III. GRAVITINO DECAY

In order to study the effects of unstable gravitino on BBN, it is important to understand the lifetime of the gravitino $\tau_{3/2}$ and its decay modes. Since gravitino is the gauge field for supersymmetry, gravitino couples to supercurrent and hence its interaction is unambiguously determined. Possible decay modes have, however, model dependence. In the following, we discuss how the decay rate and the branching ratios of the gravitino are calculated.

A. Interaction and two-body processes

We first briefly summarize the interactions of the gravitino.[6] Gravitino is the superpartner of graviton, and it couples to the supercurrent. The relevant part of the gravitino interaction is thus given by

[5]The Cases 1 and 2 are in the so-called "coannihilation region," while the Cases 3 and 4 are in the "focus-point region" and "Higgs funnel region," respectively.

[6]For details, see, for example, [25].

$$\mathcal{L}_{\rm int} = -\frac{1}{8M_*}\sum_G \bar{\lambda}^{(G)}\gamma_5\gamma^\mu[\gamma^\rho, \gamma^\sigma]\psi_\mu F^{(G)}_{\rho\sigma} - \frac{1}{\sqrt{2}M_*}\sum_C[\bar{\chi}^{(C)}\gamma^\mu\gamma^\nu P_L\psi_\mu D_\nu\phi^{(C)} + \text{H.c.}], \tag{3.1}$$

where the sum over G is for all the gauge multiplets (consisting of the gauge field $A^{(G)}_\mu$ and the gaugino $\lambda^{(G)}$) while C for the chiral multiplets (consisting of the scalar boson $\phi^{(C)}$ and the fermion $\chi^{(C)}$).[7] Here, $F^{(G)}_{\rho\sigma}$ is the field strength for $A^{(G)}_\mu$, and D_ν represents the covariant derivative. In addition, $M_* \simeq 2.4\times 10^{18}$ GeV is the reduced Planck scale. As is obvious from Eq. (3.1), if we restrict ourselves to consider the two-body final states, the gravitino decays into some standard model particle and its superpartner.

From the Lagrangian given in Eq. (3.1), we can read off the vertex factors for the gravitino and calculate the (partial) decay rates of the gravitino. We first consider the decay processes with two-body final states. Then, the decay rate is expressed as

$$\Gamma_{\rm gauge} = \frac{\beta_{\rm f} N_{\rm C}}{16\pi m_{3/2} M_*^2}\times\overline{|\mathcal{M}|^2}, \tag{3.2}$$

where $\mathcal{M}$ represents the Feynmann amplitude for the decay process (with $M_* = 1$), and $N_{\rm C}$ is the color factor: $N_{\rm C} = 8$ for the process $\psi_\mu \to g\tilde{g}$, $N_{\rm C} = 3$ for the processes with quark and squark final state, and $N_{\rm C} = 1$ otherwise. In addition, for the process $\psi_\mu \to AB$, $\beta_{\rm f}$ is given by

$$\beta_{\rm f} = \frac{1}{m_{3/2}^2}[m_{3/2}^4 - 2m_{3/2}^2(m_A^2 + m_B^2) + (m_A^2 - m_B^2)^2]^{1/2}, \tag{3.3}$$

where m_A and m_B are masses of A and B, respectively.

For the gravitino decay process into a gauge boson V and a fermion χ (i.e., chargino or neutralino), we define p, q, and q' to be the four momenta of ψ_μ, V, and χ, respectively. Then, we obtain

$$pq = \tfrac{1}{2}(m_{3/2}^2 + m_V^2 - m_\chi^2), \tag{3.4}$$

$$pq' = \tfrac{1}{2}(m_{3/2}^2 - m_V^2 + m_\chi^2), \tag{3.5}$$

$$qq' = \tfrac{1}{2}(m_{3/2}^2 - m_V^2 - m_\chi^2), \tag{3.6}$$

where m_V and m_χ are masses of V and χ, respectively. With these quantities, for the process with a massless gauge field in the final state (i.e., $\psi_\mu \to \gamma\chi_i^0$ and $g\tilde{g}$), we obtain

$$\overline{|\mathcal{M}|^2}_{\gamma,g} = \frac{2}{3}(C_L^{(\rm G)}C_L^{(\rm G)*} + C_R^{(\rm G)}C_R^{(\rm G)*})\times\left[\frac{(pq)^2(pq')}{m_{3/2}^2} + (pq)(qq')\right], \tag{3.7}$$

while with massive gauge field in the final state (i.e., $\psi_\mu \to Z\chi_i^0$ and $W^\pm\chi_i^\mp$), we obtain

$$\begin{aligned}\overline{|\mathcal{M}|^2}_{W^\pm,Z} =& \frac{2}{3}(C_L^{(\rm G)}C_L^{(\rm G)*} + C_R^{(\rm G)}C_R^{(\rm G)*})\left[\frac{(pq)^2(pq')}{m_{3/2}^2} + (pq)(qq') - \frac{1}{2}m_V^2(pq')\right] - (C_L^{(\rm G)}C_R^{(\rm G)*} + C_R^{(\rm G)}C_L^{(\rm G)*})m_{3/2}m_\chi m_V^2 \\ &+ \frac{2}{3}(C_L^{(\rm G)}C_L^{(\rm H)*} - C_R^{(\rm G)}C_R^{(\rm H)*} + \text{H.c.})m_{3/2}\left[\frac{1}{2}(qq') + \frac{(pq)(pq')}{m_{3/2}^2}\right] + (C_L^{(\rm G)}C_R^{(\rm H)*} - C_R^{(\rm G)}C_L^{(\rm H)*} + \text{H.c.})m_\chi(pq) \\ &+ \frac{2}{3}(C_L^{(\rm H)}C_L^{(\rm H)*} + C_R^{(\rm H)}C_R^{(\rm H)*})\left[1 + \frac{(pq)^2}{2m_{3/2}^2m_V^2}\right](pq') + \frac{2}{3}(C_L^{(\rm H)}C_R^{(\rm H)*} + C_R^{(\rm H)}C_L^{(\rm H)*})\left[1 + \frac{(pq)^2}{2m_{3/2}^2m_V^2}\right]m_{3/2}m_\chi.\end{aligned} \tag{3.8}$$

Here, $C_L^{(\rm G)}$, $C_R^{(\rm G)}$, $C_L^{(\rm H)}$, and $C_R^{(\rm H)}$ are vertex factors. These vertex factors for individual processes are given in Appendix A. For the decay processes with a scalar boson in the final state, we identify p, q, and q' to be the momenta of ψ_μ, scalar boson ϕ, and fermion χ, respectively. Then, the products of the momenta can be obtained from Eqs. (3.4), (3.5), and (3.6) by replacing $m_V \to m_\phi$, with m_ϕ being the mass of the scalar boson. Then, we obtain

$$\overline{|\mathcal{M}|^2}_{\rm scalar} = \frac{1}{3}\left[\frac{(pq)^2}{m_{3/2}^2} - m_\phi^2\right][(C_L^{(\rm C)}C_L^{(\rm C)*} + C_R^{(\rm C)}C_R^{(\rm C)*})\times(pq') + (C_L^{(\rm C)}C_R^{(\rm C)*} + C_R^{(\rm C)}C_L^{(\rm C)*})m_{3/2}m_\chi]. \tag{3.9}$$

The vertex factors $C_L^{(\rm C)}$ and $C_R^{(\rm C)}$ are also given in Appendix A.

B. Three-body processes

In this paper, we consider the case where the LSP is the lightest neutralino χ_1^0. Then, the two-body process

[7] $\chi^{(C)}$ represents a chiral fermion, and this should be distinguished from the charginos $\chi_i^\pm$ and neutralinos χ_i^0.

$\psi_\mu \to \gamma\chi_1^0$ is always allowed, and the (total) decay rate of the gravitino is determined by the two-body process(es). In studying the effects of the gravitino on the BBN, however, it is also important to understand the spectrum of the hadrons produced by the decay of the gravitino.

In most of the cases, the number of the hadrons from the gravitino decay is mostly determined by the two-body processes. For example, if the gravitino can decay into a superparticle other than the LSP, the emitted superparticle decays into χ_1^0. In this secondary decay process, a sizable number of the hadrons may be produced. In addition, when the mass difference between the gravitino and the lightest neutralino is larger than m_Z, the decay process $\psi_\mu \to Z\chi_1^0$ becomes kinematically allowed. In this case, the decay of the Z-boson produces a large amount of the hadrons. In most of the cases, the number of the hadrons produced from those two-body processes is much larger than that from the three-body processes. Then, the three-body processes are irrelevant for our study.

However, in some cases, precise determination of the hadron spectrum requires the calculation of the three-body final-state processes. In particular, the three-body processes become important if (i) $m_{3/2} - m_{\chi_1^0} < m_Z$, and (ii) all the superparticles except χ_1^0 and sleptons are heavier than the gravitino. Notice that, when the condition (i) is satisfied, it may be the case that the only possible two-body decay process is $\psi_\mu \to \gamma\chi_1^0$ and hence the hadrons are not produced by the two-body process. In some cases, gravitino may also decay into the lepton and slepton pair, but the decays of the (s)leptons do not produce significant amount of hadrons in our case. Thus, we pay particular attention to the process $\psi_\mu \to q\bar{q}\chi_1^0$ when $m_{3/2} - m_{\chi_1^0} < m_Z$.

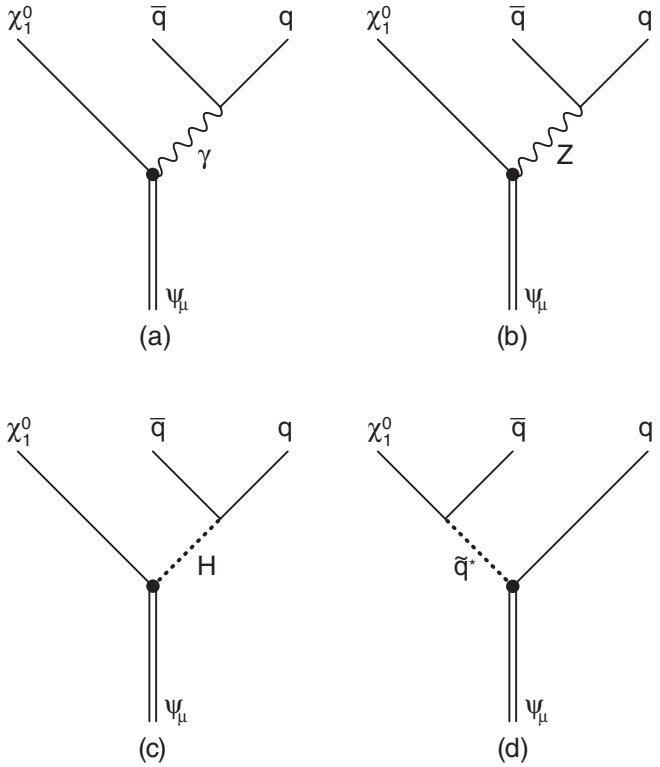

FIG. 1. Feynman diagrams for the process $\psi_\mu \to q\bar{q}\chi_1^0$. The "blobs" are from the gravitino-supercurrent interaction. For (d), there is also a CP-conjugated diagram (with the replacements $q \leftrightarrow \bar{q}$ and $\tilde{q}^* \to \tilde{q}$).

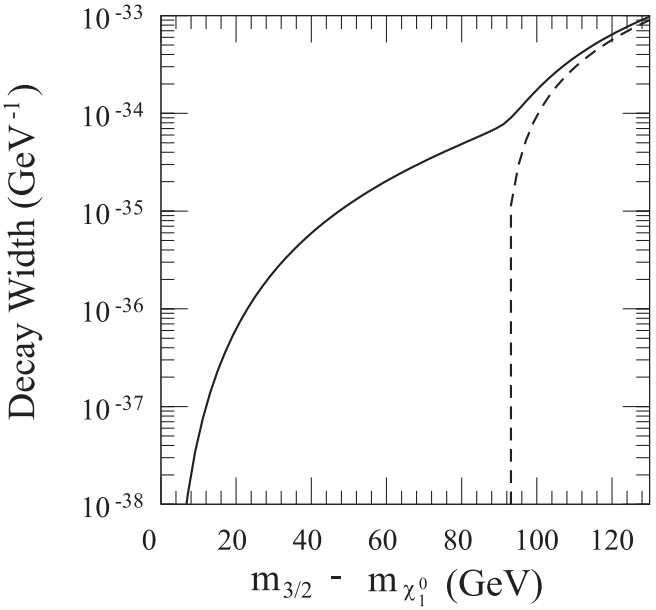

FIG. 2. Width for the process $\psi_\mu \to q\bar{q}\chi_1^0$ as a function of $m_{3/2} - m_{\chi_1^0}$ (solid line). We adopt the mSUGRA parameters for the Case 1. For comparison, the decay rate $\Gamma(\psi_\mu \to Z\chi_1^0) \times \mathrm{Br}(Z \to q\bar{q})$ is also shown in the dashed line.

When the LSP is the neutralino, the relevant three-body processes are induced by the diagrams shown in Fig. 1. In our study, we consider the effects of all the diagrams listed in Fig. 1 and calculate the decay rate for the process $\psi_\mu \to q\bar{q}\chi_1^0$. To see the importance of the three-body process, in Fig. 2, we plot the "three-body hadronic decay width" defined as[8]

$$\begin{aligned}\Gamma(\psi_\mu \to q\bar{q}\chi_1^0) \equiv\ & \Gamma(\psi_\mu \to u\bar{u}\chi_1^0) + \Gamma(\psi_\mu \to d\bar{d}\chi_1^0) \\ & + \Gamma(\psi_\mu \to s\bar{s}\chi_1^0) + \Gamma(\psi_\mu \to c\bar{c}\chi_1^0) \\ & + \Gamma(\psi_\mu \to b\bar{b}\chi_1^0) + \Gamma(\psi_\mu \to t\bar{t}\chi_1^0).\end{aligned} \tag{3.10}$$

In Fig. 2, the MSSM parameters are taken to be those for the Case 1. In this case, the three-body decay is induced dominantly by the photon-mediated diagram. When the

[8]As we discuss in the following, the three-body process becomes important when the mass difference between the gravitino and the LSP is smaller than m_Z. Thus, the process $\psi_\mu \to t\bar{t}\chi_1^0$ is not important for our analysis.

mass difference between the gravitino and the LSP becomes larger than m_Z, however, Z-boson mediated contribution with $m_{q\bar{q}} \simeq m_Z$ becomes the most important, where $m_{q\bar{q}}$ is the invariant mass of the $q\bar{q}$ system. In fact, such a process should rather be classified into the two-body process $\psi_\mu \to Z\chi_1^0$ followed by $Z \to q\bar{q}$. To see this more explicitly, we also plot the quantity $\Gamma(\psi_\mu \to Z\chi_1^0) \times \mathrm{Br}(Z \to q\bar{q})$. As one can see, $\Gamma(\psi_\mu \to q\bar{q}\chi_1^0)$ is well approximated by $\Gamma(\psi_\mu \to Z\chi_1^0) \times \mathrm{Br}(Z \to q\bar{q})$ when the decay process $\psi_\mu \to Z\chi_1^0$ becomes kinematically allowed.

In our numerical study, we treat the process $\psi_\mu \to q\bar{q}\chi_1^0$ in the following way:

(i) When $m_{3/2} - m_{\chi_1^0} < m_Z$, we calculate the Feynman diagrams shown in Fig. 1 and calculate the decay rate $\Gamma(\psi_\mu \to q\bar{q}\chi_1^0)$. (In this case, the decay process $\psi_\mu \to Z\chi_1^0$ is kinematically forbidden and hence is irrelevant.)

(ii) When $m_{3/2} - m_{\chi_1^0} > m_Z$, we approximate the hadronic decay rate induced by the diagrams in Fig. 1 by $\Gamma(\psi_\mu \to Z\chi_1^0) \times \mathrm{Br}(Z \to q\bar{q})$.

With our treatment, the effects of the photon-mediated diagram (as well as those from Figs. 1(c) and 1(d)) is neglected when $m_{3/2} - m_{\chi_1^0} > m_Z$. However, the effects of such a diagram are subdominant since the process is mainly induced by the Z-boson mediated diagram.

When $m_{3/2} - m_{\chi_1^0} > m_Z$, energy distribution of the quark and antiquark is easily calculated since the decay is dominated by the process with $m_{q\bar{q}} \simeq m_Z$. When $m_{3/2} - m_{\chi_1^0} < m_Z$, on the contrary, $m_{q\bar{q}}$ has broader distribution. Thus, in this case, we numerically calculate the differential decay rate

$$\frac{d\Gamma(\psi_\mu \to q\bar{q}\chi_1^0)}{dm_{q\bar{q}}^2}$$

to obtain the energy distributions of the quarks and antiquarks emitted from the three-body processes. (In the calculation of $d\Gamma(\psi_\mu \to q\bar{q}\chi_1^0)/dm_{q\bar{q}}^2$, we approximated that the final-state q and $\bar{q}$ have isotropic distribution in their center-of-mass frame.) The hadron spectrum from the three-body decay process is obtained by using this differential decay rate. When $m_{3/2} - m_{\chi_1^0} < m_Z$, the photon-mediated diagram gives the dominant contribution while the effects of other diagrams are almost irrelevant (unless $m_{3/2} - m_{\chi_1^0}$ is very close to m_Z). In Appendix B, we present the approximated formula of the differential decay rate, only taking account of the photon-mediated diagram.

C. Lifetime and branching ratios of the gravitino

Now we can quantitatively discuss the decay rates of the gravitino. First, following the procedures discussed in the previous subsections, we calculate the partial decay rates of the gravitino for all the possible decay modes. Adding all the contributions, we obtain the lifetime of the gravitino:

$$\tau_{3/2} = \frac{1}{\Gamma(\psi_\mu \to \mathrm{all})}. \tag{3.11}$$

We calculate $\tau_{3/2}$ as a function of the gravitino mass for the cases listed in Table II, and the results are shown in Fig. 3. The lifetime of the gravitino becomes shorter as the gravitino becomes heavier.

As one can see, when the gravitino mass is smaller than a few TeV, $\tau_{3/2}$ for the Case 4 is found to be longer than those for other cases. This is due to the fact that, for the Case 4, masses of the MSSM particles are larger than other cases and hence the decay rates of the gravitino in this case is suppressed. When the gravitino is much heavier than the MSSM particles, on the contrary, the lifetime of the gravitino is insensitive to the mass spectrum of the MSSM particles.

Importantly, when the gravitino is lighter than $\sim$20 TeV, $\tau_{3/2}$ becomes longer than 1 sec and hence the relic gravitinos decay after the BBN starts. Thus, in this case, significant constraints on the reheating temperature after inflation is expected.

Branching ratios of the decay process of the gravitino depend on the model parameters. To see this, for the Cases 1–4, we plot the branching ratios for the various two-body final states in Fig. 4. As one can see, the branching ratios have sizable model dependence when the gravitino mass is relatively small. This is because, when the gravitino mass is small, the decay rate of the gravitino is sensitive to the mass spectrum of the superparticles. When $m_{3/2}$ becomes large enough, on the contrary, branching ratios become insensitive to the model parameters.

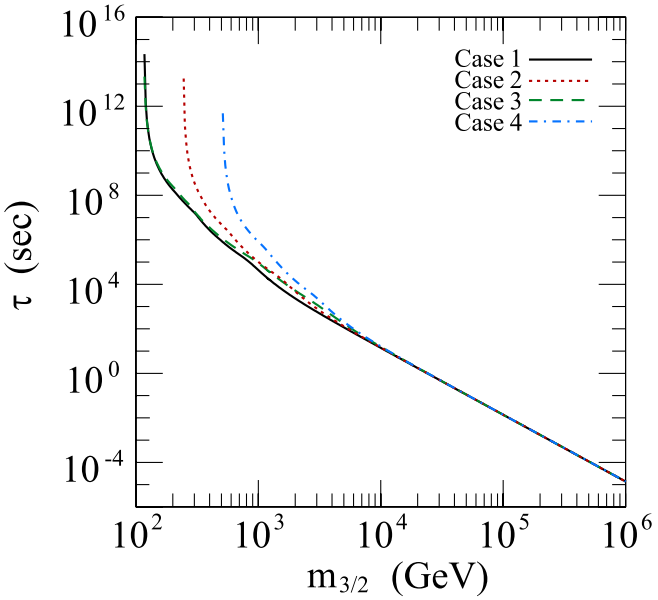

FIG. 3 (color online). Lifetime of the gravitino as a function of the gravitino mass.

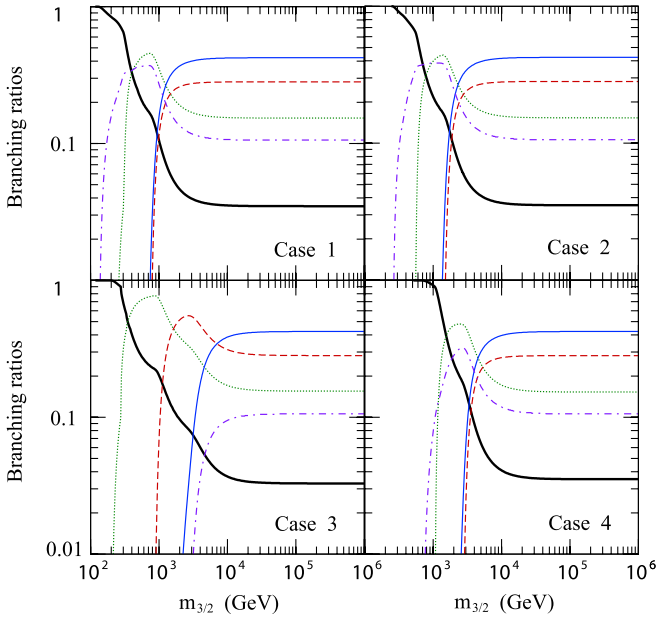

FIG. 4 (color online). Branching ratios of the decay of the gravitino as functions of the gravitino mass. The thick solid line is for the final states $\chi_1^0 +$ anything, dot-dashed line for lepton-slepton pairs, dotted line for χ_i^0 ($i = 2$–4), or chargino + anything, dashed line for gluon-gluino pair, and thin solid line for quark-squark pair final states.

IV. SECONDARY DECAYS AND HADRONIZATION

Although the gravitino primarily decays into a standard model particle and its superpartner (or into the $q\bar{q}\chi_1^0$ final state), most of the daughter particles also decay with time scale much shorter than the cosmological time scale. In addition, all the partons (i.e., quarks and gluon) are hadronized into mesons or baryons. These processes are important in the study of BBN with primordial gravitinos and, in this section, we discuss these issues.

The possible decay modes of the individual superparticles strongly depend on the mass spectrum as well as on the mixing and coupling parameters. In order to systematically take account of all the relevant decay processes, we use ISAJET package [26] which automatically calculates the partial decay rates of all the unstable particles.

In order to discuss the hadrodissociations induced by the gravitino decay, we should first calculate the spectra of the partons (i.e., u, d, s, c, b, t and their antiparticles, and gluon). There are two types of processes producing energetic partons: one is the decay of the gravitino and the other is the subsequent decays of the daughter particles. Spectra of the partons of the first type are directly calculated by using the partial decay rates of the gravitino presented in the previous section. (Here, the effects of the "three-body" processes are also included when $m_{3/2} - m_{\chi_1^0} < m_Z$.) In order to calculate the contribution of the second type, we have to follow the decay chain of the unstable particles. In addition, the parton spectra should be calculated by averaging over all the possible decay processes with the relevant branching ratios of individual particles. In our analysis, the decay chain is followed by using PYTHIA package [27] which automatically takes into account the decay processes of the unstable particles (including the superparticles).

At the cosmic time relevant for BBN, the time scale for the hadronization is much shorter than the time scale for the scattering processes and hence all the partons are hadronized before scattering off the background particles. Thus, it is necessary to calculate the spectrum of the mesons and baryons produced from the partons. In particular, for our analysis of the BBN-related processes, proton, neutron, and charged pions play significant roles.

In our analysis, the hadronization processes are dealt with PYTHIA package [27]; we have modified PYTHIA package to include the primary decay processes of the gravitino, then the subsequent decay processes of the daughter particles (including the superparticles) and the hadronization processes of the emitted partons are automatically followed by the original PYTHIA algorithm. In Fig. 5, we plot the distribution functions of the proton and neutron as functions of their kinetic energy (i.e. $E_{\rm kin} = E - m_N$ with m_N being the corresponding nucleon mass). In order to check the reliability of our estimate of the hadron spectrum, we have performed an independent calculation using ISAJET package [26]; we have also modified ISAJET package to include the decay processes of the gravitino and we calculated the hadron spectrum. We have checked that the difference between the two calculations is within 10% level. In particular, for the region with relatively large kinetic energy, which gives the most important effects on the hadrodissociation processes of the light elements, the difference is very small.

Before closing this section, we define one important parameter, which is (averaged) visible energy emitted from the gravitino decay. Once a high energy particle with electromagnetic interaction is injected into the ther-

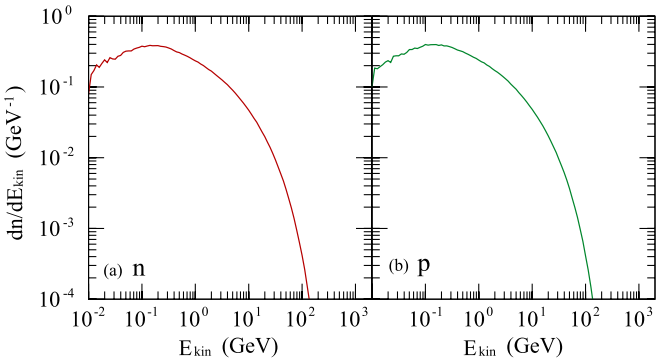

FIG. 5 (color online). Distributions of the nucleons (i.e., (a) proton and (b) neutron) from the decay of a single gravitino as functions of the kinetic energy. Here we take the mSUGRA parameters for the Case 1, and $m_{3/2} = 1$ TeV.

mal bath, it induces electromagnetic shower and, consequently, the photodissociation processes of the light elements are induced by energetic photons in the shower. The event rates of the photodissociation processes (for a fixed background temperature) are mostly determined by the total amount of the ''visible'' energy injected into the thermal bath [6]. Since we consider the case where the R-parity is conserved, some fraction of the energy is always carried away by the LSP for the decay process of the gravitino. Taking account of such effect, we calculate the averaged visible energy emitted by a single decay of the gravitino[9]:

$$E_{\rm vis} = m_{3/2} - \langle E_{\chi_1^0} \rangle - \langle E_\nu \rangle, \tag{4.1}$$

where the second and third terms of the right-hand side are the (averaged) energy carried away by the LSP and the neutrinos, respectively. $E_{\rm vis}$ is used for the calculations of the photodissociation rates.

V. LIGHT-ELEMENT ABUNDANCES

A. Theoretical calculation

Now, we explain how we calculate the light-element abundances. In order to set a bound on the reheating temperature after inflation, we assume that gravitinos are produced by scattering processes of the thermal particles. Using the thermally averaged gravitino production cross section given in [28], the ''yield variable'' of the gravitino, which is defined as $Y_{3/2} \equiv \frac{n_{3/2}}{s}$, is given by [16]

$$Y_{3/2} \simeq 1.9 \times 10^{-12} \left(\frac{T_{\rm R}}{10^{10}\ {\rm GeV}} \right) \left[1 + 0.045 \ln \left(\frac{T_{\rm R}}{10^{10}\ {\rm GeV}} \right) \right] \times \left[1 - 0.028 \ln \left(\frac{T_{\rm R}}{10^{10}\ {\rm GeV}} \right) \right], \tag{5.1}$$

where $n_{3/2}$ is the number density of the gravitino while $s = \frac{2\pi^2}{45} g_{*S}(T) T^3$ is the entropy density with $g_{*S}(T)$ being the effective number of the massless degrees of freedom at the temperature T, and the reheating temperature is defined as[10]

$$T_{\rm R} \equiv \left(\frac{10}{g_* \pi^2} M_*^2 \Gamma_{\rm inf}^2 \right)^{1/4}, \tag{5.2}$$

with $\Gamma_{\rm inf}$ being the decay rate of the inflaton. For $T_{\rm R} = 10^5$–10^{10} GeV, it is checked that Eq. (5.1) reproduces the exact gravitino abundance obtained by numerically solving the Boltzmann equation with an accuracy better than $\sim 5\%$.

Once produced, gravitinos decay with a very long lifetime. In particular, if the gravitino mass is smaller than ~ 20 TeV, gravitinos decay after the BBN starts and hence the light-element abundances may be significantly affected. In order to study the BBN processes with unstable gravitino, our study proceeds as follows:

(1) MSSM parameters are determined for one of the mSUGRA points given in Table II. Then, all the mass eigenvalues and mixing parameters are calculated.
(2) Using the parameters given above, we calculate partial decay rates of the gravitino for all the kinematically allowed two-body processes. When $m_{3/2} - m_{\chi_1^0} < m_Z$, we also calculate $\Gamma(\psi_\mu \to q\bar{q}\chi_1^0)$.
(3) We perform a Monte Carlo analysis using the branching ratios of the gravitino to calculate the energy distribution of the hadrons produced by the decay of the gravitino. As explained in the previous sections, the decay chain of the decay products (including the superparticles) and the hadronizations of the emitted partons are followed by the modified PYTHIA code. Simultaneously, we calculate the (averaged) emitted visible energy from the decay of the gravitino.
(4) For a given reheating temperature $T_{\rm R}$, we calculate the abundance of the thermally produced gravitino using Eq. (5.1).
(5) We calculate the light-element abundances, taking account of the decay of the thermally produced gravitinos. (Standard reactions of the light elements are also included.) We use the baryon-to-photon ratio suggested by the WMAP [4]:
$$\eta = (6.1 \pm 0.3) \times 10^{-10}, \tag{5.3}$$
at the 1σ level. (Here we enlarged the lower error bar from 0.2 to 0.3 since the Monte Carlo simulation is easier if the error bar is symmetric. This does not significantly change the resultant constraints.) The baryon-to-photon ratio is related to the density parameter of the baryon as $\Omega_B h^2 = 3.67 \times 10^7 \eta$.
(6) Since the event rates of the nonstandard processes induced by the gravitino decay are proportional to the abundance of the primordial gravitinos, deviations of the light-element abundances from the standard BBN results become larger as the reheating temperature becomes higher. The resultant light-element abundances are compared with observatio-

[9]For unstable leptons and mesons (in particular, pions), we checked that their lifetimes are shorter than their mean free time. Thus, in the calculation of the visible energy, we treated them as unstable particles and hence the energy carried away by the neutrinos are not included in $E_{\rm vis}$.

[10]Strictly speaking, the ''reheating temperature'' corresponds to the maximal temperature of the last radiation dominated era. Thus, if some scalar field ϕ other than the inflaton once dominates the Universe after the inflation, the reheating temperature here is given by the same expression as Eq. (5.2) with $\Gamma_{\rm inf}$ being replaced by the decay rate of ϕ. One of the examples of such scalar fields is the curvaton [29] which provides a new origin of the cosmic density perturbations.

nal constraints and an upper bound on the reheating temperature is obtained.

Although the details of the analysis of the photo and hadrodissociation processes and $p \leftrightarrow n$ interchange are explained in [6,9,11,16], we briefly summarize several important points. Once energetic hadrons are emitted into the thermal bath in the early Universe, they induce a hadronic shower and energetic particles in the shower cause hadrodissociation processes. In addition, released visible energy from the gravitino decay eventually goes into the form of radiation which causes an electromagnetic shower. Energetic photons in the shower cause photodissociation processes. Furthermore, when the cosmic temperature is relatively high ($T \gtrsim 0.1$ MeV), $p \leftrightarrow n$ interconverting processes by nucleons and the charged pions become significant.

When the cosmic temperature is higher than 0.3 MeV, the $p \leftrightarrow n$ interconverting processes induced by the charged pions (i.e. $p + \pi^- \rightarrow n + \pi^0$ and $n + \pi^+ \rightarrow p + \pi^0$) are the most important. Since the resultant ^{4}He abundance is sensitive to the n/p ratio, such interconverting processes affect the ^{4}He abundance.

Since the charged pions are expected to be stopped in the thermal bath before interconverting the background nucleons, we need to know only the total numbers of π^+ and π^- produced by the decay of the gravitino. The number of pions produced by the decay of the single gravitino is plotted in Fig. 6 as a function of the gravitino mass for the Case 1. As one can see, the number of the pions increases as the gravitino mass becomes larger. In addition, when the gravitino mass is smaller than $\sim$1 TeV, partial decay rates of the gravitino have significant dependence on $m_{3/2}$ because the gravitino mass becomes close to the masses of the MSSM superparticles in this region; consequently, the number of pions has a strong dependence on $m_{3/2}$. In the figure, we also plot the number of the proton and the neutron produced by the decay of the gravitino.

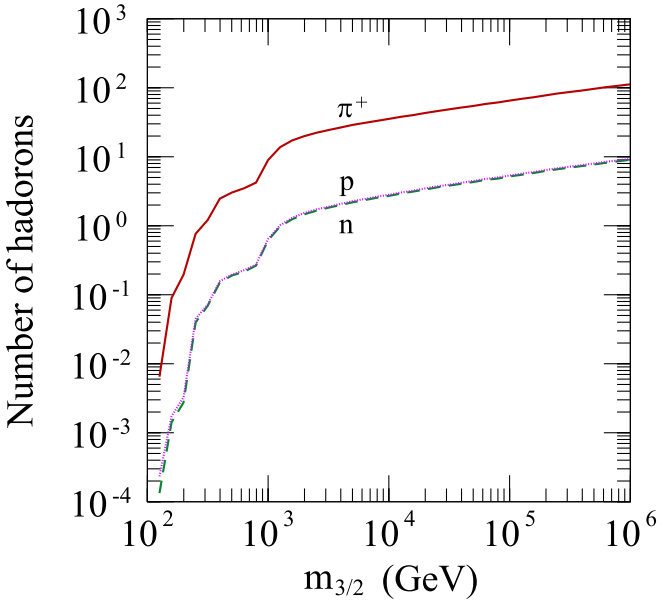

FIG. 6 (color online). Number of hadrons(π, p, n) produced by the decay of single gravitino for the Case 1. (The number of π^- is the same as that of π^+ within the expected error of the Monte Carlo analysis.)

As the lifetime of the gravitino becomes longer, it is likely that most of the thermally produced gravitinos decay after ^{4}He and other light elements (like D, T, ^{3}He, and so on) are synthesized. Then, the hadro and photodissociation processes may significantly change the light-element abundances.

When 10^2 sec $\lesssim \tau_{3/2} \lesssim 10^7$ sec, hadrodissociation processes of the light elements are important while, for longer lifetime, photodissociation processes give more significant constraints. In particular, since the number density of ^{4}He is much larger than those of other light elements, dissociation of ^{4}He may significantly change the abundances of D and ^{3}He. In addition, nonthermally produced T and ^{3}He may scatter off the background ^{4}He to produce ^{6}Li via the processes T + ^{4}He $\rightarrow$ ^{6}Li + p and ^{3}He + ^{4}He $\rightarrow$ ^{6}Li + n [10,11,15,16]. Since there is a very stringent upper bound on the primordial abundance of ^{6}Li, such nonthermal production of ^{6}Li gives a significant constraint on the reheating temperature.

B. Observational constraints

In order to derive a bound on the reheating temperature, we compare the theoretical results of the light-element abundances with observational constraints. The observational constraints we use are summarized below. Since there are uncertainties in the constraints, we adopt several different bounds on the primordial abundances of the light elements in some cases. The errors of the following observational values are at 1σ level unless otherwise stated. When we adopt both the statistical and systematic errors, we add them in quadrature.

For the D abundance, we use constraints obtained from the measurements in high redshift quasi-stellar object (QSO) absorption systems [30]. Here, we consider two constraints; one is the "averaged" constraint

$$(n_{\rm D}/n_{\rm H})^{\rm obs} = (2.78^{+0.44}_{-0.38}) \times 10^{-5}, \qquad (5.4)$$

while the other is the "conservative" one, which is the highest value of $n_{\rm D}/n_{\rm H}$ among the results listed in [30]:

$$(n_{\rm D}/n_{\rm H})^{\rm obs} = (3.98^{+0.59}_{-0.67}) \times 10^{-5}. \qquad (5.5)$$

(Here and hereafter, the superscript "obs" is used for primordial values inferred by observations.)

Abundance of ^{3}He may significantly change during evolution of the Universe from the BBN epoch to the present epoch. Thus, for ^{3}He, it is not easy to observationally determine its primordial value. In our analysis, we do not rely on any detailed model of chemical evolution to derive bound on the primordial abundance of ^{3}He. Instead,

we only use the fact that D is more fragile than ^{3}He [31]. Then, we expect that the ratio $r_{3,2} \equiv n_{^3\mathrm{He}}/n_{\mathrm{D}}$ does not decrease with time [15–17,32]. The solar-system value of ^{3}He-to-D ratio is measured as [33]

$$r^{\odot}_{3,2} = 0.59 \pm 0.54 \quad (2\sigma). \tag{5.6}$$

Thus, we obtain the upper bound on the primordial ^{3}He to D ratio

$$r^{\mathrm{obs}}_{3,2} \leq r^{\odot}_{3,2}. \tag{5.7}$$

For the primordial abundance of ^{4}He, we use the constraints from the recombination lines from low metallicity extragalactic HII regions. Taking into account the fact that several groups independently derived bounds on the mass fraction of ^{4}He, we derive upper bounds on T_{R} with the following three different bounds: the first one is based on the analysis by Fields and Olive [34]

$$Y^{\mathrm{obs}}(\mathrm{FO}) = 0.238 \pm (0.002)_{\mathrm{stat}} \pm (0.005)_{\mathrm{syst}}, \tag{5.8}$$

where the first and second errors are the statistical and systematic ones, respectively, the second is obtained by Izotov and Thuan [35]:

$$Y^{\mathrm{obs}}(\mathrm{IT}) = 0.242 \pm (0.002)_{\mathrm{stat}}(\pm(0.005)_{\mathrm{syst}}), \tag{5.9}$$

where we have added the systematic errors following Refs. [36–38], and the last one is by Olive and Skillman [39]:

$$Y^{\mathrm{obs}}(\mathrm{OS}) = 0.249 \pm 0.009, \tag{5.10}$$

where the error includes both the statistical and systematic ones. With these three constraints, we will discuss how the upper bound on T_{R} changes as we adopt different values of Y^{obs}.

The primordial value of ^{7}Li abundance is observed in old Pop II halo stars. Typically $n_{^7\mathrm{Li}}/n_{\mathrm{H}}$ is $O(10^{-10})$. In [40], it was reported that

$$(n_{^7\mathrm{Li}}/n_{\mathrm{H}})^{\mathrm{obs}} = 1.23^{+0.68}_{-0.32} \times 10^{-10}, \tag{5.11}$$

while, recently, relatively higher value of ^{7}Li abundance was also reported [41]:

$$\log_{10}[(n_{^7\mathrm{Li}}/n_{\mathrm{H}})^{\mathrm{obs}}] = -9.66 \pm (0.056)_{\mathrm{stat}} \pm (0.06)_{\mathrm{syst}}. \tag{5.12}$$

Here, ^{7}Li abundances given in Eqs. (5.11) and (5.12) differ by the factor $\sim$2, and we expect that there is still some large uncertainty for the observational values of $n_{^7\mathrm{Li}}/n_{\mathrm{H}}$. Here, we adopt the constraint given in [41] with an additional large systematic error, considering the possibilities of the increase by the cosmic-ray spallation of the C, N, O, and so on, and the decrease by the depletion by the convection in the stars [42]

$$\log_{10}[(n_{^7\mathrm{Li}}/n_{\mathrm{H}})^{\mathrm{obs}}] = -9.66 \pm (0.056)_{\mathrm{stat}} \pm (0.300)_{\mathrm{add}}. \tag{5.13}$$

The linear-scale value is given by $(n_{^7\mathrm{Li}}/n_{\mathrm{H}})^{\mathrm{obs}} = (0.54\text{–}8.92) \times 10^{-10}$ at the 2σ level. In deriving the upper bound on T_{R}, we use the constraint (5.13).

Usually the abundance of ^{6}Li is measured as a ratio of ^{6}Li and ^{7}Li in the old Pop II halo stars; at the 2σ level, $(n_{^6\mathrm{Li}}/n_{^7\mathrm{Li}})^{\mathrm{halo}} = 0.05 \pm 0.02$ [43]. The primordial value is expected to be smaller than this value because it is likely that the cosmic-ray spallation has produced additional ^{6}Li after BBN [44–46]. By adopting the milder value of the constraint on $n_{^7\mathrm{Li}}/n_{\mathrm{H}}$ given in Eq. (5.13), we get the upper bound on the primordial value of $n_{^6\mathrm{Li}}/n_{\mathrm{H}}$ at the 2σ level,

$$(n_{^6\mathrm{Li}}/n_{\mathrm{H}})^{\mathrm{obs}} < (1.10^{+5.14}_{-0.94}) \times 10^{-11}(2\sigma). \tag{5.14}$$

We use this value as the upper bound on $n_{^6\mathrm{Li}}/n_{\mathrm{H}}$ except in Sec. VI B.

VI. NUMERICAL RESULTS

A. Upper bound on T_{R}

Now, we are at the position to show our numerical results. As discussed in the previous sections, we calculate the light-element abundances as functions of the gravitino mass, other MSSM parameters, and the reheating temperature T_{R}. Then, we compare the theoretical prediction with the observations. In order to systematically derive the upper bound, we calculate the χ^2 variable defined as

$$\chi^2_i = \frac{(\bar{x}^{\mathrm{th}}_i - \bar{x}^{\mathrm{obs}}_i)^2}{(\sigma^{\mathrm{th}}_i)^2 + (\sigma^{\mathrm{obs}}_i)^2} \quad \text{for } x_i = (n_{\mathrm{D}}/n_{\mathrm{H}}), Y, \tag{6.1}$$

where $\bar{x}^{\mathrm{th}}_i$ and $\bar{x}^{\mathrm{obs}}_i$ are the center values of x_i determined from the theoretical calculation and observations, while σ^{th}_i and σ^{obs}_i are their errors, respectively. In our analysis,

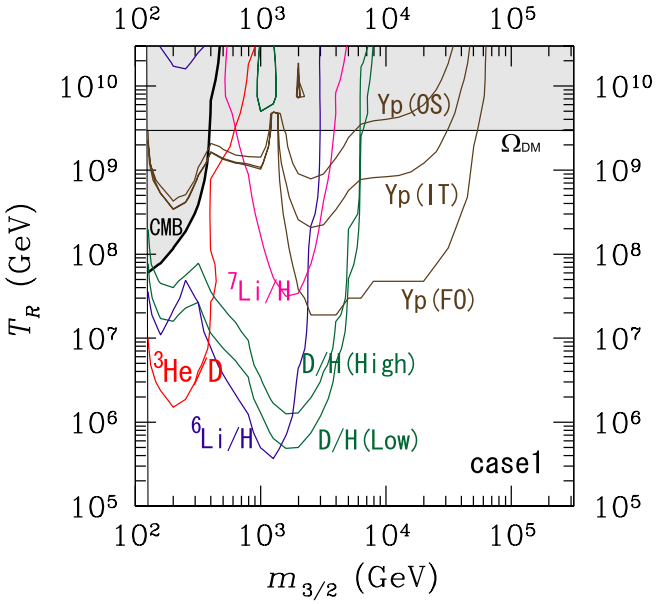

FIG. 7 (color online). Upper bound on the reheating temperature for the Case 1 as a function of the gravitino mass.

$(\sigma_i^{\rm th})^2$ is calculated by the Monte Carlo analysis. For $x_i = r_{3,2}$, $(n_{^6{\rm Li}}/n_{\rm H})$ and $\log_{10}[(n_{^7{\rm Li}}/n_{\rm H})]$ we only use the upper bound, and we define χ_i^2 as[11]

$$\chi_i^2 = \begin{cases} \frac{(\bar{x}_i^{\rm th} - \bar{x}_i^{\rm obs})^2}{(\sigma_i^{\rm th})^2 + (\sigma_i^{\rm obs})^2} & : \bar{x}_i^{\rm th} > \bar{x}_i^{\rm obs} \text{ for } x_i = r_{3,2}, (n_{6{\rm Li}}/n_{\rm H}), \log_{10}[(n_{7{\rm Li}}/n_{\rm H})] \\ 0 & : \text{otherwise} \end{cases}. \tag{6.2}$$

Then, we derive 95% level constraints for each observational constraint; with the probability distributions obtained from Eqs. (6.1) and (6.2), 95% level constraint is given by $\chi_i^2 = 3.84$ and $\chi_i^2 = 2.71$, respectively.[12]

In Figs. 7–10, we show the upper bounds on the reheating temperature. For D, we considered the observational constraints (5.4) and (5.5) to see how the upper bound depends on the bound on D. For ^{3}He, ^{7}Li, and ^{6}Li, we use (5.6), (5.13), and (5.14), respectively. For ^{4}He, we consider three cases (5.8) (FO), (5.9) (IT), (5.10) (OS), since the upper bound on $T_{\rm R}$ for the case of relatively heavy gravitino is sensitive to the observational constraint on the abundance of ^{4}He. In deriving Figs. 7–10, the MSSM parameters are determined by using the mSUGRA parameters given in Table II. In addition, the lifetime of the gravitino as well as its branching ratios are calculated using the MSSM mass spectrum obtained from these parameters. In this analysis, we concentrated on the case where the gravitino is unstable. In the figures, we shaded the region where $m_{3/2} < m_{\chi_1^0}$.

Although we have considered four different cases with different mass spectrum of the MSSM particles, the qualitative behavior of the constraints are quite insensitive to the choice of underlying parameters. When the gravitino mass is larger than a few TeV, most of the primordial gravitinos decay at a very early stage of BBN. In this case, photo and hadrodissociations are ineffective. The overproduction of ^{4}He due to $p \leftrightarrow n$ conversion becomes the most important. For the observational constraints on the mass fraction of ^{4}He, we consider three different observational results given in Eqs. (5.8), (5.9), and (5.10). As one can see, the upper bound on $T_{\rm R}$ in this case is sensitive to the observational constraint on the primordial abundance of ^{4}He; for the case of $m_{3/2} = 10$ TeV, for example, $T_{\rm R}$ is required to be lower than 3×10^7 GeV if we use the lowest value of Y given in Eq. (5.8) while, with the highest value given in Eq. (5.10), the upper bound on the reheating temperature becomes as large as 4×10^9 GeV.

When 400 GeV $\lesssim m_{3/2} \lesssim$ 5 TeV, gravitinos decay when the cosmic temperature is 1–100 keV. In this case, hadrodissociation gives the most stringent constraints; in particular, the overproductions of D and ^{6}Li become important. Furthermore, when the gravitino mass is relatively light ($m_{3/2} \lesssim 400$ GeV), the most stringent constraint is from the ratio ^{3}He/D which may be significantly changed by photodissociation of ^{4}He.

It should be noted that, even when the gravitino cannot directly decay into colored particles (i.e. the squarks, gluino, and their superpartners) due to a kinematical reason, the reheating temperature may still be stringently constrained from the hadrodissociation processes. This is

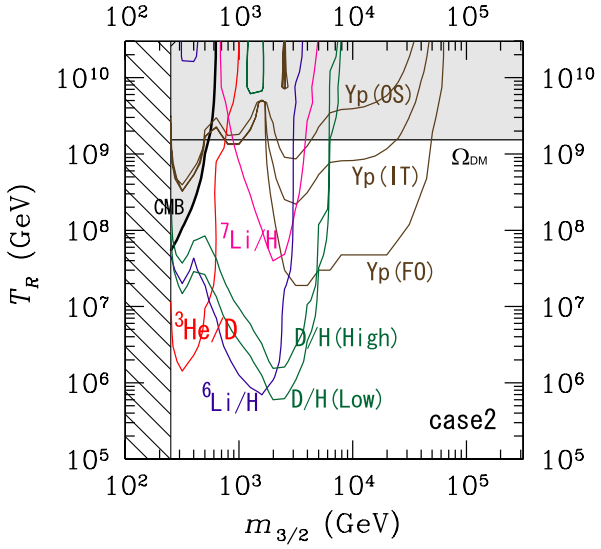

FIG. 8 (color online). Same as Fig. 7 except for the MSSM parameters are evaluated for the Case 2.

[11]For $n_{^7{\rm Li}}$, we only use the upper bound since we could not include one of the nonthermal production processes of $n_{^7{\rm Li}}$: $N + \alpha_{\rm BG} \to N + \alpha + \pi's$, followed by $\alpha + \alpha_{\rm BG} \to {\rm L^7i} + \cdots$. This is due to the lack of some experimental data. (For details, see [16], and also the next subsection.) In addition, in Refs. [9,11], the ratio $n_{^6{\rm Li}}/n_{^7{\rm Li}}$ was used in order to constrain the primordial abundance of ^{6}Li. In our analysis, because of the potential uncertainty in $n_{^7{\rm Li}}$, we use the ratio $n_{^6{\rm Li}}/n_{\rm H}$ instead of $n_{^6{\rm Li}}/n_{^7{\rm Li}}$.

[12]For the probability distribution given in Eq. (6.1), we consider normal Gaussian probability distribution to obtain 95% level constraints, which corresponds to $\chi^2 \le 3.84$. For the case with Eq. (6.2), we assumed that (normalized) probability density is given in the form of

$$P_i(x_i) = \frac{1}{\sqrt{2\pi[(\sigma_i^{\rm th})^2 + (\sigma_i^{\rm obs})^2]}} \exp\left[\frac{(x_i - \bar{x}_i^{\rm obs})^2}{2(\sigma_i^{\rm th})^2 + 2(\sigma_i^{\rm obs})^2}\right].$$

Then, we set the 95% level upper bound on the primordial quantity x_i, which we denote $x_i^{\rm (max)}$, by the relation

$$\int_{-\infty}^{x_i^{\rm (max)}} P_i(x_i) dx_i = 0.95,$$

which gives $\chi_i^2 = 2.71$ with Eq. (6.2). Notice that, in Eq. (6.2), the χ^2 variable is set to be 0 when $\bar{x}_i^{\rm th} \le \bar{x}_i^{\rm obs}$ in order to derive an upper bound. We have checked that the χ^2 variable varies very steeply as the reheating temperature changes. Thus, the upper bounds shown in the following figures do not change much even if we slightly change the upper bound on χ^2.

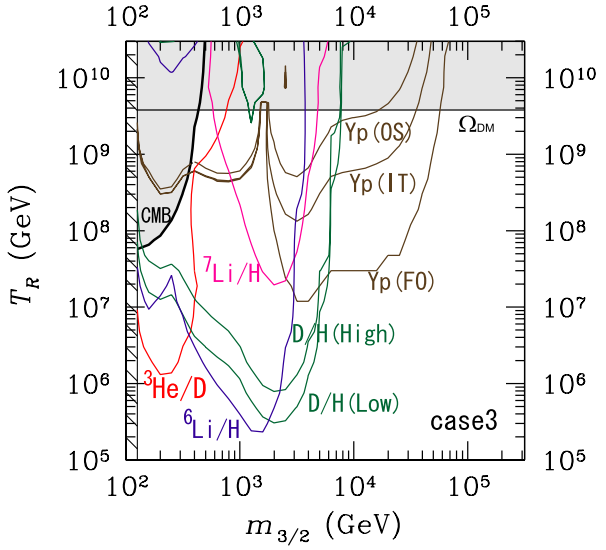

FIG. 9 (color online). Same as Fig. 7 except for the MSSM parameters are evaluated for the Case 3.

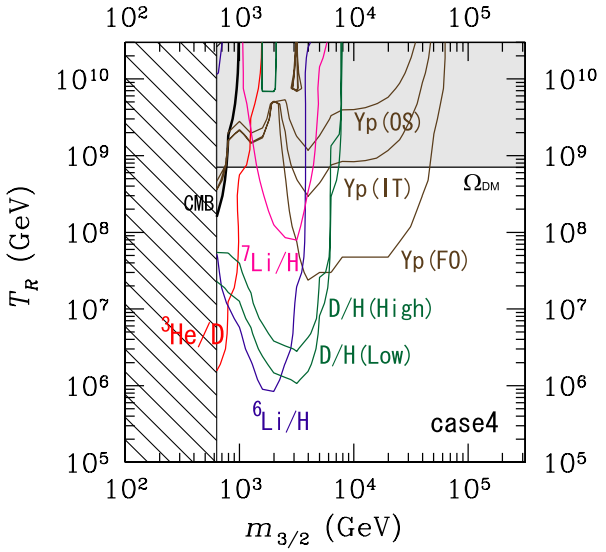

FIG. 10 (color online). Same as Fig. 7 except for the MSSM parameters are evaluated for the Case 4.

due to the fact that some of noncolored decay products (in particular, the weak bosons $W^{\pm}$ and Z as well as some of the superparticles) produce hadrons when they decay. In particular, when the mass difference $m_{3/2} - m_{\chi_1^0}$ is larger than m_Z, hadrodissociations become important since a sizable amount of hadrons are produced by the process $\psi_\mu \to Z\chi_1^0$.

Although Figs. 7–10 look roughly the same, the upper bound on the reheating temperature has model dependences. In particular, for a fixed value of the gravitino mass, the upper bound depends on the MSSM parameters as one can see in the figures. To see this in more detail, in Table III, we show the upper bound on T_R for the cases listed in Table II. For the fixed value of the gravitino mass, the upper bound on T_R may vary by the factor as large as $\sim$10 when the gravitino mass is of the order of 1 TeV. When the gravitino becomes heavier than $\sim$10 TeV, however, the upper bound becomes insensitive to the model parameters. This is due to the fact that, in this case, the branching ratios of the gravitino are almost independent of the MSSM parameters.

Model dependence of the upper bound on the reheating temperature is mostly from the change of the lifetime and decay modes. For the Case 1, we have chosen the mSUGRA parameters which give relatively light superparticles (compared to other cases). In the Case 2, masses of all the superparticles are slightly increased compared to the Case 1. Consequently, we can see some changes of the constraints on the reheating temperature.

Compared to the Case 1, scalar masses are significantly increased in the Case 3 with the gaugino masses being unchanged. In this case, gravitino is likely to decay into gauginos, in particular, into gluino when kinematically allowed. (See Fig. 4.) We found that the gluon-gluino final state produces more hadrons (in particular, protons and neutrons) than the quark-squark final state. Consequently, in the Case 3, upper bound on T_R becomes lower than that for the Case 2. We have also studied the case where masses of all the squarks and sfermions are pushed to infinity by hand while keeping the gaugino masses as low as $O(100\ \mathrm{GeV})$. In this case, the constraint on T_R is almost the same as that for the Case 3. In addition, in the Case 4, masses of all the superparticles are very large ($\sim$ a few

TABLE III. Upper bound on T_R for several values of the gravitino mass. For the D, ^{3}He, and ^{6}Li abundances, here we use the observational constraints (5.4), (5.6), and (5.14). For ^{4}He, we consider three cases (5.8) (FO), (5.9) (IT), (5.10) (OS).

$m_{3/2}$	Case 1	Case 2	Case 3	Case 4
300 GeV	6×10^6 GeV	3×10^6 GeV	4×10^6 GeV	...
1 TeV	5×10^5 GeV	1×10^6 GeV	4×10^5 GeV	6×10^6 GeV
3 TeV	1×10^6 GeV	1×10^6 GeV	4×10^5 GeV	1×10^6 GeV
10 TeV (FO)	3×10^7 GeV	3×10^7 GeV	2×10^7 GeV	3×10^7 GeV
10 TeV (IT)	8×10^8 GeV	8×10^8 GeV	6×10^8 GeV	8×10^8 GeV
10 TeV (OS)	4×10^9 GeV	4×10^9 GeV	3×10^9 GeV	4×10^9 GeV

TeV). Then, the lifetime of the gravitino becomes relatively long, which makes the upper bound less stringent for gravitinos with $m_{3/2} \sim$ a few TeV.

Although our main concern is to study the effects of the gravitino decay on BBN, it is also important to consider other constraints. One of the important constraints is from the production of the LSP from the decay of the gravitino. Importantly, the LSP is produced with the decay of the gravitino, and the present number density of the LSP is given by the sum of two contributions; the thermal relic, which is calculated with DarkSUSY package for each case, and the nonthermally produced LSP from the gravitino decay. Since one LSP is produced by the decay of one gravitino, the density parameter of the LSP which has nonthermal origin is given by[13]

$$\Delta\Omega_{\rm LSP}h^2 \simeq 0.054 \times \left(\frac{m_{\chi_1^0}}{100\ {\rm GeV}}\right)\left(\frac{T_{\rm R}}{10^{10}\ {\rm GeV}}\right), \quad (6.3)$$

where we have neglected the logarithmic corrections in Eq. (5.1). If we require, for example, that the total mass density of the LSP be within the 95% C.L. bound of the WMAP constraint (i.e. $(\Omega_{\rm LSP}^{\rm (thermal)} + \Delta\Omega_{\rm LSP})h^2 < 0.1287$ [4]), we also obtain upper bound on $T_{\rm R}$, which is given by 3×10^9 GeV, 2×10^9 GeV, 4×10^9 GeV, and 7×10^8 GeV, for the Cases 1, 2, 3, and 4, respectively.[14] In our numerical analysis, we calculated the abundance of the LSP taking account of the entropy production by the decay of the gravitino; constraint from $\Delta\Omega_{\rm LSP}$ is also shown in the figures.

Another constraint may be obtained from the distortion of the cosmic microwave background (CMB). Additional injection of photons into the thermal bath by decaying particles is severely constrained in order not to disturb the black-body shape of the CMB spectrum [47,48]; numerically, $|\mu| < 9 \times 10^{-5}$ for μ-distortion and $|y| < 1.5 \times 10^{-5}$ for y-distortion are required [49]. Using these constraints, we obtain the upper bound on the total amount of the injected energy $\Delta\rho_\gamma$; using the relation $\Delta\rho_\gamma/s = E_{\rm vis}Y_{3/2}$,

$$\frac{\Delta\rho_\gamma}{s} < 1.60 \times 10^{-13}\ {\rm GeV} \times \left(\frac{\tau_{3/2}}{10^{10}\ {\rm sec}}\right)^{-1/2} \times \exp[(\tau_{\rm dC}/\tau_{3/2})^{5/4}], \quad (6.4)$$

for μ-distortion for $\tau_{\rm dC} \lesssim \tau_{3/2} \lesssim 2.5 \times 10^9$ sec $\times(\Omega_b h^2/0.022)$ [48], with $\tau_{\rm dC}$ being decoupling time of the double Compton scattering:

$$\tau_{\rm dC} = 6.10 \times 10^6\ {\rm sec} \times \left(\frac{T_0}{2.725\ {\rm K}}\right)^{-12/5}\left(\frac{\Omega_b h^2}{0.022}\right)^{4/5} \times \left(\frac{1 - Y_p/2}{0.88}\right)^{4/5}, \quad (6.5)$$

and

$$\frac{\Delta\rho_\gamma}{s} < 2.7 \times 10^{-13}\ {\rm GeV} \times \left(\frac{\tau_{3/2}}{10^{10}\ {\rm sec}}\right)^{-1/2}, \quad (6.6)$$

for y-distortion for $\tau_{3/2} \gtrsim 2.5 \times 10^9$ sec $\times(\Omega_b h^2/0.022)$ [47]. Here T_0 is the photon temperature at present. Constraint from the distortion of the CMB spectrum is also shown in the figures.

B. Comment on the ^{7}Li abundance

So far, we have considered constraints on the reheating temperature, assuming that the prediction of standard BBN agrees with observations. Although standard BBN predicts light-element abundances which are more or less consistent with the observational constraints, however, it has been pointed out that, if we adopt the baryon-to-photon ratio suggested by the WMAP, standard BBN predicts the ^{7}Li abundance slightly larger than the observed value. Indeed, if we do not include the additional systematic error added in Eq. (5.13), the standard BBN prediction is found to be more than 2σ away from the center value. If we take this discrepancy seriously, we need some explanation which may include some effect of particle-physics model beyond the standard model [17,50–52]. Before closing this section, we comment on this issue.

If the net production of ^{7}Li can be somehow suppressed by the decay of the long-lived particle (like the gravitino), the ^{7}Li discrepancy may be solved. In the past, it was discussed that the ^{7}Li abundance may be reduced by the photodissociation process induced by the *radiative* decay of the long-lived particle [50]. The scenario with a long-lived particle which decays only radiatively is, however, severely constrained by the ^{3}He constraint; in such a scenario, photodissociation of background ^{4}He is also induced which overproduces ^{3}He. Thus, such a scenario does not work once the constraint on the ^{3}He abundance is taken into account [9,11,32].

In order to solve the discrepancy, recently it was pointed out that the suppression of the ^{7}Li abundance may be possible with *hadronically* decaying long-lived particles. In [14], it was discussed that, when the lifetime of the long-lived particle is $\sim 10^3$ sec, abundance of ^{7}Li can become consistent with the observational constraint (with no additional systematic error) without conflicting other constraints. The reduction of ^{7}Li is mainly due to the dissociation of ^{7}Be (which decays into ^{7}Li) by slow neutrons produced in the hadronic shower. (To be more exact,

[13] In fact, entropy production occurs when the gravitino decays, and consequently, primordial LSPs are diluted by some amount. For the reheating temperature giving the constraint on the relic density of the LSP, however, the effect of the dilution is negligible.

[14] This bound is sensitive to the choice of the MSSM parameters since the abundance of the thermally produced LSPs depends on the MSSM parameter. If we choose a parameter set which gives $\Omega_{\rm LSP}^{\rm (thermal)}$ much smaller than the WMAP value, bound from the production of the LSP may become much weaker.

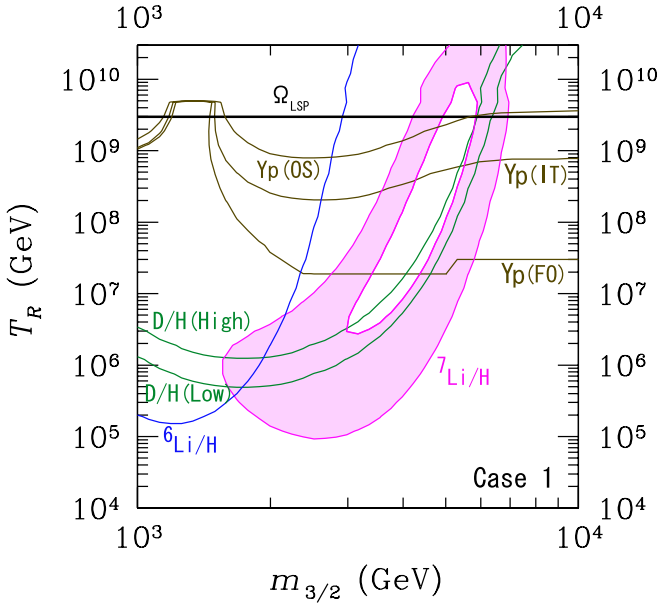

FIG. 11 (color online). Parameter region which predicts the ^{7}Li abundance consistent with (5.12); in the shaded region the ^{7}Li abundance becomes consistent with (5.12). We have used the mSUGRA parameters for the Case 1.

such slow neutrons are supplied by the destruction of ^{4}He, the interconversion from protons, and so on.)

To study this issue, we have looked for the parameter region where the ^{7}Li abundance becomes consistent with the observational constraint (5.12).[15] Although dissociation of ^{7}Be by slow neutrons, which is the most important process, is taken into account in our numerical calculation, we could not include one of nonthermal production processes of ^{7}Li: $N + \alpha_{\rm BG} \to N + \alpha + \pi's$, followed by $\alpha + \alpha_{\rm BG} \to {}^7{\rm Li} + \cdots$. This is because experimental data for the energy distribution of the final state α is not available for the first process. Thus, the ^{7}Li abundance should be somehow underestimated. However with a mild assumption that the kinetic energy of the energetic α produced by the process $N + \alpha_{\rm BG} \to N + \alpha + \pi's$ is $\sim$140 MeV in the center-of-mass system independently of the energy of the beam nucleon [53], we checked that the resultant ^{7}Li abundance is not significantly affected by this nonthermal production process in the parameter region in which we will be interested. Thus, we believe that our calculation gives a reasonable estimate of the ^{7}Li abundance (even though the lower bound on the ^{7}Li abundance was not considered in deriving the upper bound on $T_{\rm R}$).

[15]Note in this case that the χ^2 of $\log_{10}[(n_{^7{\rm Li}}/n_{\rm H})]$ is calculated by Eq. (6.1) (not Eq. (6.2)), and 95% C.L. corresponds to $\chi^2 = 3.84$. In addition, because we fix the observational value of $n_{^6{\rm Li}}/n_{^7{\rm Li}}$, and we adopt the observational value of $n_{^7{\rm Li}}/n_{\rm H}$ in (5.12), the observational constraint on $n_{^6{\rm Li}}/n_{\rm H}$ is also modified to be $(n_{^6{\rm Li}}/n_{\rm H})^{\rm obs} < (1.10^{+1.12}_{-0.56}) \times 10^{-11}$ (2σ).

In Fig. 11, we show our numerical result; in the shaded region, the ^{7}Li becomes consistent with the observational constraint (5.12). In this calculation, we have used the mSUGRA parameters for the Case 1 to determine the MSSM parameters although the result is insensitive to the choice of the mSUGRA parameters. As one can see, when $m_{3/2} \sim$ a few TeV and $T_{\rm R} \sim 10^{5-7}$ GeV ($Y_{3/2} \sim 10^{-17}$–10^{-15}), the ^{7}Li abundance becomes consistent with Eq. (5.12) without conflicting the observational constraints for other light elements. We have checked that this region is consistent with the parameter region suggested in [14]. We have also checked that we can find a parameter region which gives ^{7}Li abundance consistent with (5.11).

VII. CONCLUSIONS AND DISCUSSION

In this paper, we have studied the effects of unstable gravitino on the BBN in detail. In particular, compared to previous works, we have performed precise calculations of the decay rate and the branching ratios of the gravitino. For this purpose, we have first fixed the masses and the mixing parameters of the MSSM particles, then calculated the decay rates for all the relevant two and three-body decay processes of the gravitino. Then, we calculate the spectrum of the hadrons (in particular, p, n, and $\pi^{\pm}$). With the hadron spectrum as well as the visible energy emitted from the decay of the gravitino, we calculate the light-element abundances as functions of the gravitino mass and the reheating temperature. By comparing the results of the theoretical calculation with the observational constraints, we derived the upper bound on the reheating temperature after the inflation.

Although we have considered several different mass spectrum of the MSSM particles, resultant constraints on the reheating temperature behave qualitatively the same. The detailed bound is, however, sensitive to the mass spectrum of the superparticles and the upper bounds on $T_{\rm R}$ for several cases are summarized in Table III. When the gravitino mass is a few TeV, in particular, the hadrodissociation processes provide significant constraints. Of course, in some cases, production of the hadrons is suppressed; in particular, when the gravitino mass is close to the LSP mass, the only possible two-body decay process is $\psi_\mu \to \gamma\chi_1^0$. In this case, hadrons are produced by the three-body decay processes $\psi_\mu \to q\bar{q}\chi_1^0$, which is suppressed compared to the two-body decay process. Consequently, constraints become less stringent.

Finally, we compare the current constraints on the reheating temperature with those obtained in previous works. When the gravitino mass is so small that the lifetime becomes longer than $\sim 10^6$ sec, the most significant constraint is derived from photodissociation processes. Effects of the photodissociation processes have been studied in [9]. The upper bound derived in our paper is basically consistent with the one obtained in [9]. In fact, in [9], the mass of the LSP was neglected in calculating the spectrum of high

energy photons, which resulted in an overestimation of the number of high energy photons. Consequently, for the parameter region where the gravitino mass is close to the mass of the LSP, constraint on $T_{\rm R}$ given in our work is less stringent than that given in [9]. Effects of photodissociation were also studied in [13]. Theoretical prediction (taking account of the effects of photodissociation) of the light-element abundances differs by a factor of ~ 3 or so between our results and theirs, which may be due to the difference of high energy photon spectrum used in the calculations. In comparing the upper bound on the primordial abundance of gravitino, it should be also noted that the observational constraints on light-element abundances are different between two works; [13] adopted less stringent observational constraints than ours. (For more details, see footnote 17 of [16].)

With larger gravitino mass, hadrodissociation provides more stringent upper bounds on the reheating temperature. Since we have followed the procedure of [15,16], upper bounds obtained in those works are consistent with ours. In comparing the results, it should be noted that, in [15,16], hadron spectrum induced by the gravitino decay was calculated with some simplifications and assumptions since the main purpose of [15,16] was to discuss effects of generic late-decaying particles on BBN. Since the decay processes of gravitino were more carefully calculated in this paper, there is slight quantitative difference of the upper bound on $T_{\rm R}$ for a given gravitino mass. Effects of the hadronic decay were also studied in [14]. In particular, ^{7}Li abundance given in our calculation is consistent with that given in [14]. Results of our calculation agree with those in [14] at the qualitative level.

If the gravitino is the LSP, the gravitino becomes stable and the cosmological constraints change drastically [2,3]. A detailed study of the case of the gravitino LSP will be given elsewhere [54].

ACKNOWLEDGMENTS

This work is supported in part by the 21st Century COE program, ''Exploring New Science by Bridging Particle-Matter Hierarchy.'' The work of T. M. and K. K. is also supported by the Grants-in-Aid of the Ministry of Education, Science, Sports, and Culture of Japan No. 15540247 (T. M.) and No. 15-03605 (K. K.). K. K. is also supported by NSF Grant AST No. 0307433.

APPENDIX A: VERTEX FACTORS FOR THE GRAVITINO DECAY

In this appendix, we present the vertex factors for the decay processes of the gravitino. For the two-body decay processes with a gauge boson in the final state, the decay rate can be calculated with Eq. (3.2) with Eq. (3.7) or (3.8). The vertex factors $C_L^{(\rm G)}$, $C_R^{(\rm G)}$, $C_L^{(\rm H)}$, and $C_R^{(\rm H)}$ depend on the mixing parameters.

For $\psi_\mu \to \gamma\chi_i^0$, the vertex factors are given by

$$[C_L^{(\rm G)}]_{\psi_\mu\to\gamma\chi_i^0} = [C_R^{(\rm G)*}]_{\psi_\mu\to\gamma\chi_i^0} = \frac{1}{g_Z}(g_2[U^*_{\chi^0}]_{i1} + g_1[U^*_{\chi^0}]_{i2}), \quad \text{(A1)}$$

where g_2 and g_1 are gauge coupling constants for the $SU(2)_L$ and $U(1)_Y$ gauge group, respectively, while for the gluon-gluino final state,

$$[C_L^{(\rm G)}]_{\psi_\mu\to g\tilde{g}} = [C_R^{(\rm G)*}]_{\psi_\mu\to g\tilde{g}} = 1. \quad \text{(A2)}$$

In addition, for $\psi_\mu \to Z\chi_i^0$,

$$[C_L^{(\rm G)}]_{\psi_\mu\to Z\chi_i^0} = [C_R^{(\rm G)*}]_{\psi_\mu\to Z\chi_i^0} = \frac{1}{g_Z}(-g_1[U^*_{\chi^0}]_{i1} + g_2[U^*_{\chi^0}]_{i2}), \quad \text{(A3)}$$

$$[C_L^{(\rm H)}]_{\psi_\mu\to Z\chi_i^0} = -[C_R^{(\rm H)*}]_{\psi_\mu\to Z\chi_i^0} = \frac{1}{\sqrt{2}} g_Z(-v_1[U^*_{\chi^0}]_{i3} + v_2[U^*_{\chi^0}]_{i4}), \quad \text{(A4)}$$

and for $\psi_\mu \to W^\pm \chi_i^\mp$,

$$[C_L^{(\rm G)}]_{\psi_\mu\to W^\pm\chi_i^\mp} = [U^*_{\chi^-}]_{i1}, \quad \text{(A5)}$$

$$[C_R^{(\rm G)}]_{\psi_\mu\to W^\pm\chi_i^\mp} = [U_{\chi^+}]_{i1}, \quad \text{(A6)}$$

$$[C_L^{(\rm H)}]_{\psi_\mu\to W^\pm\chi_i^\mp} = -g_2 v_1[U^*_{\chi^-}]_{i2}, \quad \text{(A7)}$$

$$[C_R^{(\rm H)}]_{\psi_\mu\to W^\pm\chi_i^\mp} = g_2 v_2[U_{\chi^+}]_{i2}. \quad \text{(A8)}$$

For other processes, the decay rates can be calculated with Eq. (3.9). The vertex factor for the neutral Higgs emission processes ($\psi_\mu \to h\chi_i^0$, $\psi_\mu \to H\chi_i^0$, and $\psi_\mu \to A\chi_i^0$) are given by

$$[C_L^{(\rm C)}]_{\psi_\mu\to h\chi_i^0} = [C_R^{(\rm C)*}]_{\psi_\mu\to h\chi_i^0} = -\sin\alpha[U^*_{\chi^0}]_{i3} + \cos\alpha[U^*_{\chi^0}]_{i4}, \quad \text{(A9)}$$

$$[C_L^{(\rm C)}]_{\psi_\mu\to H\chi_i^0} = [C_R^{(\rm C)*}]_{\psi_\mu\to H\chi_i^0} = \cos\alpha[U^*_{\chi^0}]_{i3} + \sin\alpha[U^*_{\chi^0}]_{i4}, \quad \text{(A10)}$$

$$[C_L^{(\rm C)}]_{\psi_\mu\to A\chi_i^0} = -[C_R^{(\rm C)*}]_{\psi_\mu\to A\chi_i^0} = \sin\beta[U^*_{\chi^0}]_{i3} + \cos\beta[U^*_{\chi^0}]_{i4}, \quad \text{(A11)}$$

while, for $\psi_\mu \to H^\pm \chi_i^\mp$,

$$[C_L^{(\rm C)}]_{\psi_\mu\to H^\pm\chi_i^\mp} = \sqrt{2}\sin\beta[U^*_{\chi^-}]_{i2}, \quad \text{(A12)}$$

$$[C_R^{(\rm C)}]_{\psi_\mu\to H^\pm\chi_i^\mp} = \sqrt{2}\cos\beta[U_{\chi^+}]_{i2}, \quad \text{(A13)}$$

respectively. For the rest of the processes (with a quark or a lepton in the final state),

$$[C_L^{(\mathrm{C})}]_{\psi_\mu \to f\tilde{f}_i} = \sqrt{2}[U_{\tilde{f}}^{-1}]_{Li}, \tag{A14}$$

$$[C_R^{(\mathrm{C})}]_{\psi_\mu \to f\tilde{f}_i} = \sqrt{2}[U_{\tilde{f}}^{T}]_{Ri}. \tag{A15}$$

APPENDIX B: APPROXIMATED FORMULA FOR THREE-BODY PROCESS

Even though there are several diagrams contributing to the three-body decay process of the gravitino $\psi_\mu \to q\bar{q}\chi_1^0$, photon-mediated diagram, Fig. 1(a), plays the most important role when $m_{3/2} - m_{\chi_1^0} < m_Z$; indeed, in this case, the decay rate $\Gamma(\psi_\mu \to q\bar{q}\chi_1^0)$ is well approximated by the results only with Fig. 1(a). Thus, although we have calculated all the relevant diagrams for the three-body processes in our numerical study, we present the approximated formula for the differential decay rate for the three-body process, which is given by

$$\frac{d\Gamma(\psi_\mu \to q\bar{q}\chi_1^0)}{dm_{q\bar{q}}^2 dm_{q\chi_1^0}^2} \simeq \frac{d\Gamma(\psi_\mu \to \gamma^*\chi_1^0 \to q\bar{q}\chi_1^0)}{dm_{q\bar{q}}^2 dm_{q\chi_1^0}^2} = \frac{N_{\mathrm{C}}}{256\pi^3 m_{3/2}^3 M_*^2} \times \overline{|\mathcal{M}|^2}, \tag{B1}$$

where $N_{\mathrm{C}} = 3$. In addition, $m_{q\bar{q}}^2$ and $m_{q\chi_1^0}^2$ are the invariant masses of the $q\bar{q}$ and $q\chi_1^0$ systems, respectively, and are in the following range

$$(2m_q)^2 \le m_{q\bar{q}}^2 \le (m_{3/2} - m_{\chi_1^0})^2, \tag{B2}$$

$$(m_q + m_{\chi_1^0})^2 \le m_{q\chi_1^0}^2 \le (m_{3/2} - m_q)^2, \tag{B3}$$

$$m_{3/2}^2 + m_{\chi_1^0}^2 + 2m_q^2 - (m_{3/2} - m_q)^2 \le m_{q\bar{q}}^2 + m_{q\chi_1^0}^2 \le m_{3/2}^2 + m_{\chi_1^0}^2 + 2m_q^2 - (m_q + m_{\chi_1^0})^2, \tag{B4}$$

with m_q being the mass of the final-state quark. The photon-mediated three-body decay amplitude is given by

$$\overline{|\mathcal{M}|^2} = \frac{4}{3}\frac{e^2 Q_q^2}{m_{q\bar{q}}^2}(C_L^{(\mathrm{G})} C_L^{(\mathrm{G})*} + C_R^{(\mathrm{G})} C_R^{(\mathrm{G})*}) \tag{B5}$$

$$\left\{\left[(kq')(kp) + (k'q')(k'p) - 2m_q^2\left((pq') - \frac{(pq)(qq')}{m_{q\bar{q}}^2}\right)\right]\right. \tag{B6}$$

$$+ \frac{(pq')}{m_{3/2}^2}\left[(pk)^2 + (pk')^2 + 2\frac{m_q^2 (pq)^2}{m_{q\bar{q}}^2}\right] - m_{3/2} m_{\chi_1^0}(m_{q\bar{q}}^2 + 2m_q^2)\Big\}, \tag{B7}$$

where p, q', k, k', q are the momenta of ψ_μ, χ_1^0, q, $\bar{q}$, and intermediate photon γ^*, respectively. Furthermore, $C_L^{(\mathrm{G})}$, $C_R^{(\mathrm{G})}$ are defined in Appendix A, and eQ_q is the electric charge of q.

As discussed in Sec. III, when $m_{3/2} - m_{\chi_1^0} > m_Z$, the process $\psi_\mu \to q\bar{q}\chi_1^0$ is mostly mediated by the process with on-shell Z-boson, and hence $\Gamma(\psi_\mu \to q\bar{q}\chi_1^0)$ is well approximated by $\Gamma(\psi_\mu \to Z\chi_1^0) \times \mathrm{Br}(Z \to q\bar{q})$.

[1] S. Weinberg, Phys. Rev. Lett. **48**, 1303 (1982).
[2] T. Moroi, H. Murayama, and M. Yamaguchi, Phys. Lett. B **303**, 289 (1993).
[3] J. L. Feng, A. Rajaraman, and F. Takayama, Phys. Rev. Lett. **91**, 011302 (2003); Phys. Rev. D **68**, 063504 (2003); J. L. Feng, S. f. Su, and F. Takayama, Phys. Rev. D **70**, 063514 (2004); L. Roszkowski and R. Ruiz de Austri, J. High Energy Phys. 08 (2005) 080; K. Jedamzik, M. Lemoine, and G. Moultaka, Phys. Rev. D **73**, 043514 (2006).
[4] C. L. Bennett *et al.*, Astrophys. J. Suppl. Ser. **148**, 1 (2003); D. N. Spergel *et al.*, Astrophys. J. Suppl. Ser. **148**, 175 (2003).
[5] D. Lindley, Astrophys. J. **294**, 1 (1985); M. Y. Khlopov and A. D. Linde, Phys. Lett. B **138**, 265 (1984); J. R. Ellis, J. E. Kim, and D. V. Nanopoulos, Phys. Lett. B **145**, 181 (1984); R. Juszkiewicz, J. Silk, and A. Stebbins, Phys. Lett. B **158**, 463 (1985); J. R. Ellis, D. V. Nanopoulos, and S. Sarkar, Nucl. Phys. **B259**, 175 (1985); J. Audouze, D. Lindley, and J. Silk, Astrophys. J. **293**, L53 (1985); D. Lindley, Phys. Lett. B **171**, 235 (1986); M. Kawasaki and K. Sato, Phys. Lett. B **189**, 23 (1987); R. J. Scherrer and M. S. Turner, Astrophys. J. **331**, 19 (1988); J. R. Ellis, G. B. Gelmini, J. L. Lopez, D. V. Nanopoulos, and S. Sarkar, Nucl. Phys. **B373**, 399 (1992).
[6] M. Kawasaki and T. Moroi, Prog. Theor. Phys. **93**, 879 (1995); Astrophys. J. **452**, 506 (1995).
[7] M. Kawasaki and T. Moroi, Phys. Lett. B **346**, 27 (1995).
[8] R. J. Protheroe, T. Stanev, and V. S. Berezinsky, Phys. Rev. D **51**, 4134 (1995).
[9] E. Holtmann, M. Kawasaki, K. Kohri, and T. Moroi, Phys. Rev. D **60**, 023506 (1999).
[10] K. Jedamzik, Phys. Rev. Lett. **84**, 3248 (2000).
[11] M. Kawasaki, K. Kohri, and T. Moroi, Phys. Rev. D **63**, 103502 (2001).
[12] K. Kohri, Phys. Rev. D **64**, 043515 (2001).
[13] R. H. Cyburt, J. R. Ellis, B. D. Fields, and K. A. Olive, Phys. Rev. D **67**, 103521 (2003).

[14] K. Jedamzik, Phys. Rev. D **70**, 063524 (2004).
[15] M. Kawasaki, K. Kohri, and T. Moroi, Phys. Lett. B **625**, 7 (2005).
[16] M. Kawasaki, K. Kohri, and T. Moroi, Phys. Rev. D **71**, 083502 (2005).
[17] J. R. Ellis, K. A. Olive, and E. Vangioni, Phys. Lett. B **619**, 30 (2005).
[18] N. Okada and O. Seto, Phys. Rev. D **71**, 023517 (2005).
[19] K. Kohri, M. Yamaguchi, and J. Yokoyama, Phys. Rev. D **70**, 043522 (2004); **72**, 083510 (2005).
[20] M. H. Reno and D. Seckel, Phys. Rev. D **37**, 3441 (1988).
[21] S. Dimopoulos, R. Esmailzadeh, L. J. Hall, and G. D. Starkman, Astrophys. J. **330**, 545 (1988); Phys. Rev. Lett. **60**, 7 (1988); Nucl. Phys. **B311**, 699 (1989).
[22] H. E. Haber and G. L. Kane, Phys. Rep. **117**, 75 (1985).
[23] S. P. Martin, hep-ph/9709356.
[24] P. Gondolo *et al.*, J. Cosmol. Astropart. Phys. 07 (2004) 008.
[25] T. Moroi, hep-ph/9503210.
[26] The ISAJET homepage: http://www.phy.bnl.gov/~isajet/.
[27] PYTHIA webpage: http://www.thep.lu.se/~torbjorn/Pythia.html.
[28] M. Bolz, A. Brandenburg, and W. Buchmuller, Nucl. Phys. **B606**, 518 (2001).
[29] K. Enqvist and M. S. Sloth, Nucl. Phys. **B626**, 395 (2002); D. H. Lyth and D. Wands, Phys. Lett. B **524**, 5 (2002); T. Moroi and T. Takahashi, Phys. Lett. B **522**, 215 (2001); **539**, 303(E) (2002); Phys. Rev. D **66**, 063501 (2002).
[30] D. Tytler, X. m. Fan, and S. Burles, Nature (London) **381**, 207 (1996); S. Burles and D. Tytler, Astrophys. J. **499**, 699 (1998); **507**, 732 (1998); J. M. O'Meara *et al.*, Astrophys. J. **552**, 718 (2001); M. Pettini and D. V. Bowen, Astrophys. J. **560**, 41 (2001); D. Kirkman *et al.*, Astrophys. J. Suppl. Ser. **149**, 1 (2003).
[31] R. I. Epstein, J. M. Lattimer, and D. N. Schramm, Nature (London) **263**, 198 (1976).
[32] G. Sigl, K. Jedamzik, D. N. Schramm, and V. S. Berezinsky, Phys. Rev. D **52**, 6682 (1995).
[33] J. Geiss, *Origin and Evolution of the Elements*, edited by N. Prantzos, E. Vangioni-Flam, and M. Cassé (Cambridge University Press, Cambridge, England, 1993), p. 89.
[34] B. D. Fields and K. A. Olive, Astrophys. J. **506**, 177 (1998).
[35] Y. I. Izotov and T. X. Thuan, Astrophys. J. **602**, 200 (2004).
[36] K. A. Olive and G. Steigman, Astrophys. J. Suppl. Ser. **97**, 49 (1995).
[37] K. A. Olive, E. Skillman, and G. Steigman, Astrophys. J. **483**, 788 (1997).
[38] Y. I. Izotov, T. X. Thuan, and V. A. Lipovetsky, Astrophys. J. Suppl. Ser. **108**, 1 (1997).
[39] K. A. Olive and E. D. Skillman, Astrophys. J. **617**, 29 (2004).
[40] S. G. Ryan, J. Norris, and T. C. Beers, Astrophys. J. **523**, 654 (1999); S. G. Ryan *et al.*, Astrophys. J. Lett. **530**, L57 (2000).
[41] P. Bonifacio *et al.*, Astron. Astrophys. **390**, 91 (2002).
[42] B. D. Fields, K. Kainulainen, K. A. Olive, and D. Thomas, New Astron. Rev. **1**, 77 (1996).
[43] V. V. Smith, D. L. Lambert, and P. E. Nissen, Astrophys. J. **408**, 262 (1993); L. M. Hobbs and J. A. Thorburn, Astrophys. J. **491**, 772 (1997); V. V. Smith, D. L. Lambert, and P. E. Nissen, Astrophys. J. **506**, 405 (1998); R. Cayrel *et al.*, Astron. Astrophys. **343**, 923 (1999).
[44] D. K. Duncan, D. L. Lambert, and M. Lemke, Astrophys. J. **401**, 584 (1992); M. Cassé, R. Lehoucq, and E. Vangioni-Flam, Nature (London) **373**, 318 (1995); R. Ramaty, B. Kozlovsky, and R. E. Lingenfelter, Astrophys. J. Lett. **438**, L21 (1995).
[45] M. Lemoine, D. N. Schramm, J. W. Truran, and C. J. Copi, Astrophys. J. **478**, 554 (1997).
[46] B. D. Fields and K. A. Olive, New Astron. Rev. **4**, 255 (1999).
[47] J. R. Ellis, G. B. Gelmini, J. L. Lopez, D. V. Nanopoulos, and S. Sarkar, in [5].
[48] W. Hu and J. Silk, Phys. Rev. Lett. **70**, 2661 (1993).
[49] D. J. Fixsen *et al.*, Astrophys. J. **473**, 576 (1996).
[50] J. L. Feng, A. Rajaraman, and F. Takayama, in [3].
[51] K. Ichikawa and M. Kawasaki, Phys. Rev. D **69**, 123506 (2004).
[52] K. Ichikawa, M. Kawasaki, and F. Takahashi, Phys. Lett. B **597**, 1 (2004).
[53] C. Y. Wong, *Introduction To High-Energy Heavy Ion Collisions* (World Scientific, Singapore, 1994); M. Kaneta (NA44 Collaboration), Prog. Theor. Phys. Suppl. **129**, 167 (1997); Ph. D thesis, Hiroshima University, 1999.
[54] K. Kohri, T. Moroi, and A. Yotsuyanagi (unpublished).